Bumetanide increases Cl⁻-dependent short-circuit current in late distal colon: Evidence for the presence of active electrogenic Cl⁻ absorption

Lieqi Tang[1], Xiefan Fang[1], Steven P. Winesett[1], Catherine Y. Cheng[1], Henry J. Binder[2], Scott A. Rivkees[1], Sam X. Cheng[3]*

1 Department of Pediatrics, University of Florida, Gainesville, FL, United States of America, 2 Department of Internal Medicine, Yale School of Medicine, New Haven, CT, United States of America, 3 Department of Pediatrics, Gastroenterology, Hepatology, and Nutrition, University of Florida, Gainesville, FL, United States of America

* sam.cheng@ufl.edu

Abstract

Mammalian colonic epithelia consist of cells that are capable of both absorbing and secreting Cl⁻. The present studies employing Ussing chamber technique identified two opposing short-circuit current (I_{sc}) responses to basolateral bumetanide in rat distal colon. Apart from the transepithelial Cl⁻-secretory I_{sc} in early distal colon that was inhibited by bumetanide, bumetanide also stimulated I_{sc} in late distal colon that had not previously been identified. Since bumetanide inhibits basolateral Na⁺-K⁺-2Cl⁻ cotransporter (NKCC) in crypt cells and basolateral K⁺-Cl⁻ cotransporter (KCC) in surface epithelium, we proposed this stimulatory I_{sc} could represent a KCC-mediated Cl⁻ absorptive current. In support of this hypothesis, ion substitution experiments established Cl⁻ dependency of this absorptive I_{sc} and transport inhibitor studies demonstrated the involvement of an apical Cl⁻ conductance. Current distribution and RNA sequencing analyses revealed that this Cl⁻ absorptive I_{sc} is closely associated with epithelial Na⁺ channel (ENaC) but is not dependent on ENaC activity. Thus, inhibition of ENaC by 10 μM amiloride or benzamil neither altered the direction nor its activity. Physiological studies suggested that this Cl⁻ absorptive I_{sc} senses dietary Cl⁻ content; thus when dietary Cl⁻ was low, Cl⁻ absorptive I_{sc} was up-regulated. In contrast, when dietary Cl⁻ was increased, Cl⁻ absorptive I_{sc} was down-regulated. We conclude that an active Cl⁻ extrusion mechanism exists in ENaC-expressing late distal colon and likely operates in parallel with ENaC to facilitate NaCl absorption.

Introduction

Sodium chloride transport in mammalian colon occurs in two opposing directions: secretion and absorption. The secretory process is primarily localized to crypt cells, whereas the absorptive process is mainly present in surface cells [1, 2]. During secretion, basolateral bumetanide-

sensitive Na^+-K^+-$2Cl^-$-cotransporter (NKCC1) moves Cl^- uphill into the cell using the Na^+ electrochemical gradient generated by Na^+,K^+-ATPase (NKA); Cl^- is then transported out of the cell into the lumen via apical Cl^- channels such as cystic fibrosis transmembrane conductor regulator (CFTR), and Na^+ flows through a paracellular shunt [2]. In this secretory process, the transport of Cl^- anion is active and can be measured in an Ussing chamber as a decrease in bumetanide-sensitive short-circuit current (I_{sc}), and the transport of the counter ion Na^+ is passive, i.e., it only follows the transepithelial voltage, V_T, set up by CFTR-mediated Cl^- secretion, and is therefore not electrogenic and will not be reflected in I_{sc} measurement [2].

On the contrary, Na^+ and Cl^- movements across absorptive surface epithelium are believed to be opposite to secretion, both in direction and in sequence. Na^+ is taken up from the luminal side of the epithelium by the amiloride-sensitive epithelial Na^+ channel (ENaC), driven by the Na^+ electrochemical gradient generated by the NKA, and Na^+ is then pumped out of the cell by the basolateral NKA, and Cl^- flows passively by electrodiffusion [2]. The latter occurs either paracellularly or through a transcellular shunt pathway along a downhill driving force for Cl^- [2]. In this absorptive process, the movement of Na^+ is active and electrogenic, and can be measured in an Ussing chamber as amiloride-sensitive I_{sc} decrease, whereas the movement of Cl^- is considered passive and is solely dependent on the lumen-negative V_T generated by ENaC.

However, although passive Cl^- absorption may occur when luminal Cl^- concentration ($[Cl^-]_L$) is high, $[Cl^-]_L$ in the colon is variable, and depends on the colonic secretory rate, the Cl^- content in the diet, and the luminal concentrations of other anions. Under normal non-diarrheal conditions, $[Cl^-]_L$ in the colon is low because, under these conditions, the main luminal anions are short-chain fatty acids (SCFAs), which may have a concentration as high as 120 mM [3, 4]. Furthermore, as fluid passes along the length of colon, $[Cl^-]_L$ falls further (due to reabsorption), and when it reaches the distal colon, particularly the late distal colon, the $[Cl^-]_L$ can become extremely low (e.g., $\leq$ 10 mM [5], which is far below the estimated intracellular $[Cl^-]$ of 30–40 mM [6–8]). Therefore, under these ionic conditions passive absorption of Cl^- will not occur. This raises the question of whether an active mechanism for Cl^- absorption exists in the distal colon.

According to the aforementioned current transport model, one would expect that luminal lose dose amiloride application would inhibit ENaC and thereby reduce I_{sc} in late distal colon. This is because ENaC-mediated electrogenic Na^+ absorption is restricted to the surface epithelium in this portion of the colon [2]. One would also anticipate that serosal bumetanide treatment would inhibit NKCC1 and thereby reduce I_{sc} in both early and late distal colon, as NKCC1 that mediates the electrogenic Cl^- secretion is primarily located in crypt cells, which are present in both early and late distal colon [2, 9].

Therefore, in the present study our initial experiments were performed to examine amiloride- and bumetanide-sensitive I_{sc} responses in early and late distal colonic mucosa of rats using Ussing chamber technique [10]. We found that mucosal amiloride inhibited I_{sc} in the late distal colon and that serosal bumetanide inhibited I_{sc} in the early distal colon as predicted. Surprisingly, however, in the late distal colon serosal bumetanide caused no inhibition but I_{sc} stimulation. This positive I_{sc} response to bumetanide in the late distal colon cannot be explained by the aforementioned Cl^- secretory I_{sc} as predicted by the current model [2]; instead, it is consistent with the presence of an active Cl^- absorptive current in this portion of the colon. In agreement with this, our ion dependence studies demonstrated that this positive or stimulatory I_{sc} by bumetanide in the late distal colon was indeed a Cl^- (not Na^+ or K^+) current, and prior inhibition of ENaC with amiloride or benzamil, which diminished the lumen-negative V_T, was unable to diminish this stimulatory I_{sc} by bumetanide. Thus, these findings confirm that this Cl^- absorptive I_{sc} is neither passive nor dependent on ENaC-mediated Na^+ absorption, as previously predicted.

In an attempt to define the apical and basolateral transporters involved, in subsequent experiments we further characterized this electrogenic Cl⁻ absorptive I_{sc}, both pharmacologically using transport inhibitors and molecularly using gene differential expression analysis combined with Western blots. We also performed physiological experiments that respectively increase and decrease dietary Cl⁻ in order to explore the physiological role this electrogenic Cl⁻ absorptive I_{sc} may play in this salt-sensitive late colonic epithelium and to determine if it is up-regulated in response to decreased dietary Cl⁻ and down-regulated in response to increased dietary Cl⁻. Together, our data established that an active Cl⁻ absorptive mechanism is present in late distal colon in parallel with ENaC, and that it is actively involved in NaCl absorption when salt is in deficit.

Materials and methods

Animals and tissue preparation

Experiments were performed with non-fasting male adult Sprague-Dawley rats (5–10 week old with a body weight of 100–300 g) obtained from Charles River Laboratories. Before sacrifice, animals were subjected to one of the following three dietary treatments for a week: 1) normal salt diet (0.3% sodium and 0.5% chloride; Harlan Teklad, Madison, WI, USA; cat. no. T7012) plus tap water in drinking bottle, 2) low salt diet (0.1% sodium and 0.2% chloride; Harlan Teklad, Madison, WI, USA; cat. no. T7034) plus tap water in drinking bottle, 3) normal salt diet plus normal saline (0.9% NaCl) in drinking bottle to enhance daily salt intake. Animals were sacrificed with standard CO_2 inhalation, followed by cervical dislocation. A segment of distal colon of approximately 4–5 cm in length between the two landmark lymph nodes was excised and divided into early distal colon (the segment in proximity to the proximal lymph node), and late distal colon (the segment adjacent to the distal lymph node). The late distal colon was located approximately 1 cm from the anus. The use of animals, as well as the protocol for isolating colon tissues, was approved by the Institutional Animal Care and Use Committee (IACUC# 201507567) at the University of Florida.

Ussing chamber and short-circuit current measurements

Isolated colonic segments were rinsed with physiological Ringer solutions, and cut open along the mesenteric border, and then the serosa and muscular layers were stripped as described [11]. The resulting mucosal sheets were mounted on tissue-holding slides (window area = 0.3 cm²), placed in an Ussing chamber (Physiologic Instruments, San Diego, CA), and perfused with indicated Ringer solutions, gassed with 5% CO_2 / 95% O_2 when HCO_3^--containing solution was used or 100% O_2 when HCO_3^--free solution was used. Each side of the chamber contained 3 ml of solution and the temperature of the solution was adjusted to and maintained at 37°C by heated water-jacketed reservoirs. To facilitate comparison, in some experiments the mucosa segment was also divided longitudinally into 2 equal pieces and mounted into two separate Ussing chambers, with one piece of mucosa being used as control and the other as treatment. Tissues were voltage-clamped to zero potential difference by the application of short-circuit current (I_{sc}) (Voltage-Current Clamp, VCC MC8; Physiologic Instruments, San Diego, CA), except for brief interruption at 20-second intervals for recording of open-circuit potential (V_T, mV). Following the establishment of baseline and basal recordings, tissues were treated with bumetanide (100 μM, basolateral or apical), amiloride (10 μM, apical), barium (5 mM, apical), forskolin (500 nM, basolateral) or other indicated inhibitors, and I_{sc} responses were recorded. I_{sc} was measured in microamperes (μA) and is expressed as μA/cm². Tissue resistance (R, Ω.cm²) was calculated from Ohm's law.

Under the present experimental conditions, the changes in I_{sc} (ΔI_{sc}) in these distal colonic segments are largely reflective of electrogenic Cl$^-$, Na$^+$ and K$^+$ movements. In this study, ΔI_{sc} refers to induced steady state responses before and after drug treatment. Unless otherwise stated, $\Delta I_{sc}^{Bumetanide}$ was defined as ΔI_{sc} responses to 100 μM serosal bumetanide. $\Delta I_{sc}^{Amiloride}$ was defined as ΔI_{sc} responses to 10 μM mucosal amiloride. ΔI_{sc}^{Barium} was defined as ΔI_{sc} responses to 5 mM mucosal barium. $\Delta I_{sc(HCO3)}^{Forskolin}$ was defined as ΔI_{sc} responses to 500 nM serosal forskolin, measured in the presence of 100 μM serosal bumetanide (to inhibit Cl$^-$ current), 10 μM mucosal amiloride and 5 mM mucosal barium (to selectively inhibit Na$^+$ and K$^+$ conductance). These transport inhibitors were employed to reduce current interference from non HCO$_3^-$ conductance as described elsewhere [11–13] and to help determine the magnitude of apical CFTR anion conductance as, under present experimental conditions, forskolin-induced I_{sc} primarily reflects HCO$_3^-$ secretion mediated by apical CFTR and basolateral Na$^+$-HCO$_3^-$ cotransporter [11, 14]. A pilot study using HCO$_3^-$-free Ringer solution confirmed its primary HCO$_3^-$ dependency [mean ± SE (n) μA/cm^2 early and late distal colon $\Delta I_{sc(HCO3)}^{Forskolin}$ in presence $vs.$ absence of HCO$_3^-$ ion: 29.3 ± 4.0 (8) and 12.3 ± 1.6 (8) $vs.$ 4.6 ± 0.4 (3) and 2.6 ± 2.4 (3)**, P<0.01].

To determine ion dependency, additional experiments were performed in Cl$^-$-free, HCO$_3^-$-free, or Na$^+$-free Ringer solutions. In those experiments, tissues were bathed initially in normal Ringer solutions and then in respective Cl$^-$/HCO$_3^-$/Na$^+$-free Ringer solutions, as described [15]. I_{sc} were recorded and corrected for junction potentials before used for calculations.

Illumina transcriptomic RNA sequencing (RNA-Seq) and differential gene expression analysis

RNA-Seq libraries were prepared as described [16]. mRNA was isolated from total RNA prepared from early and late colonic mucosa of rats using NEXTflex™ Poly(A) Beads (Bioo Scientific, Austin, TX, USA). Sequencing libraries were prepared with the NEBNext® mRNA Library Prep Master Mix Set for Illumina (NEB, Ipswich, MA, USA) and the NEBNext Multiplex Oligos for Illumina (NEB). Illumina-adapted libraries were pooled at equal molar ratio and sequenced with one High Output 1×75 cycles run on a NextSeq500 sequencer (Illumina, San Diego, CA, USA).

The fastq files generated from RNA-Seq were uploaded to the UF Research Computing Galaxy instance developed by the University of Florida [16]. The data were cleaned with the FastQC program and mapped to the rat genome (rn6) with the Tophat2 tool. Differential expression (DE) of genes between early and late colonic mucosa segments was analyzed using Cufflinks [17], with Ensembl Rattus_norvegicus.Rnor_6.0.84.gtf as the reference annotation. Genes with false discovery rate (FDR) less than 0.05 and absolute fold change greater than 1.5 were considered as significant.

Western blots

Isolated early and late distal rat colonic mucosa were rinsed in Ringer buffer and lysed as previously described [18]. The lysates were briefly sonicated and were incubated at room temperature for 15 min before they were loaded onto a 6% SDS-polyacrylamide gel. After electrophoresis, proteins were transferred to nitrocellulose membranes (Bio-Rad) by electro blotting. After protein transfer, wet membranes were stained with ponceau S (Amresco, OH) for 1 minute and quickly destained in water to remove non-specific ponceau staining. The membranes were then imaged and total protein quantified using Imagelab 4.1 (Bio-Rad). After destaining in Tris-buffered saline with 0.1% Tween 20 (TBST), membranes were quenched with 5% nonfat milk in

TBST for 1 h at room temperature. Expression of KCC1 protein was detected with an affinity-purified polyclonal antibody raised against a 13-amino acid peptide corresponding to amino acid residues 998–1010 of the COOH-terminus of rat KCC1 (Alomone Labs, Israel, Cat #AKT-001). Incubation with primary antibody was made overnight in 5% nonfat milk containing TBST (1:200 dilution). After three 20-min washes at room temperature in TBST, membranes were incubated with anti-rabbit IgG secondary antibody conjugated horse radish peroxidase (1:5,000, Sigma, MO) for 1 h. Following three washes at room temperature in TBST, membranes were incubated with Clarity chemiluminescence substrate (Bio-Rad), imaged on the Chemidoc MP, and the bands detected analyzed with Imagelab 4.1. The KCC1 protein signals were normalized by ponceau S staining as a loading control as described [19]. Differential expression of KCC1 between early and late colonic mucosa segments was analyzed and expressed as fold change (late distal colon/early distal colon).

Chemicals, reagents and solutions

Polyclonal anti-KCC1 antibody was purchased from Alomone Labs, Israel. Bumetanide, amiloride, benzamil, barium, glibenclamide, 5-nitro-2-(3-phenylpropylamino)benzoic acid (NPPB), CFTR(inh)-172, and forskolin were obtained from Sigma while GlyH 101 was from Calbiochem. All stock solutions were prepared in DMSO. Normal salt diet and low salt diet were purchased from Harlan Teklad. Ringer solution contains (in mM) 140.8 Na^+, 5.2 K^+, 123.5 Cl^-, 25 HCO_3^-, 1.25 Ca^{2+}, 1.25 Mg^{2+} and 5 glucose, pH 7.4. Cl^--free Ringer solution contains HCO_3^- (25 mM) with no Cl^-. HCO_3^--free Ringer solution contains Cl^- with no HCO_3^-. Na^+-free Ringer solution contains no Na^+. In these solutions, isethionate was used in place of anion Cl^- and HCO_3^- and N-Methyl-D-glucamine (NMDG) was used as a substitute for Na^+. HCO_3^--containing solutions were gassed with 95% O_2-5% CO_2; HCO_3^--free solution was gassed with 100% O_2.

Statistical analysis

Values are expressed as means ± S.E.M. ΔI_{sc} refers to induced steady state responses before and after drug treatment. Data were analyzed by the paired or unpaired two-tailed Student's *t*-test, as appropriate, using Microsoft Excel 2010 for Windows or GraphPad Prism version 6 for Windows (GraphPad Software, San Diego, CA). $P < 0.05$ was considered significant.

Results

Bumetanide induces two opposing I_{sc} in distal colon: Inhibitory in early distal colon and stimulatory in late distal colon

The initial set of experiments was performed to assess transepithelial Cl^- secretion in the distal colon of rats by measuring short-circuit current (I_{sc}) response to basolateral bumetanide of colonic mucosa mounted in Ussing chambers. As a control, the effect of apical bumetanide was examined.

Fig 1 summarizes the effects of bumetanide on I_{sc} in early and late distal colon. Fig 1A shows representative I_{sc} responses to sequential additions of bumetanide (100 μM) to apical and basolateral chambers in early and late distal colon. Quantitative summaries are shown in Fig 1B. Without bumetanide, I_{sc} was significant larger in early than late distal colon (Table 1). The addition of bumetanide to the apical side of the epithelium had no effect on I_{sc} in either colonic segment. In contrast, the addition of bumetanide to the basolateral side significantly decreased I_{sc} in early distal colon, as predicted by the transport model for active secretion of Cl^- [2]. Surprisingly, in late distal colon, the same basolateral bumetanide treatment caused a
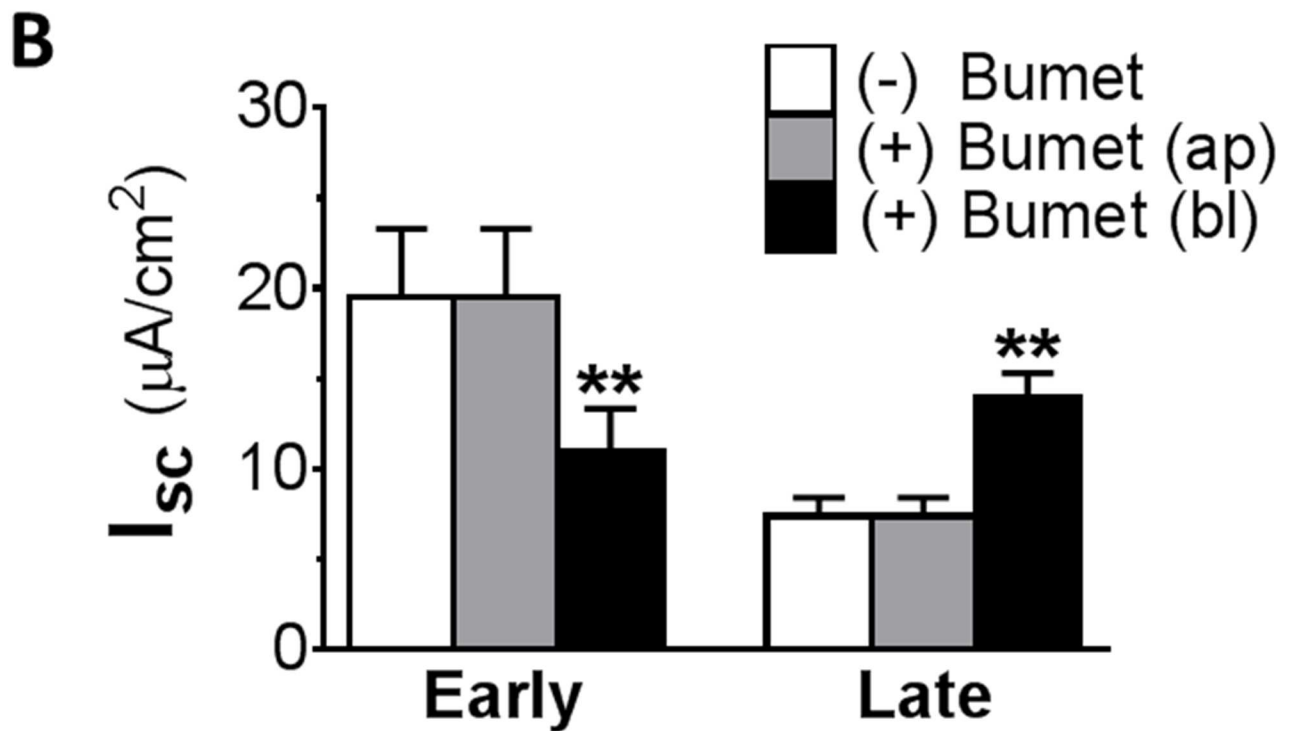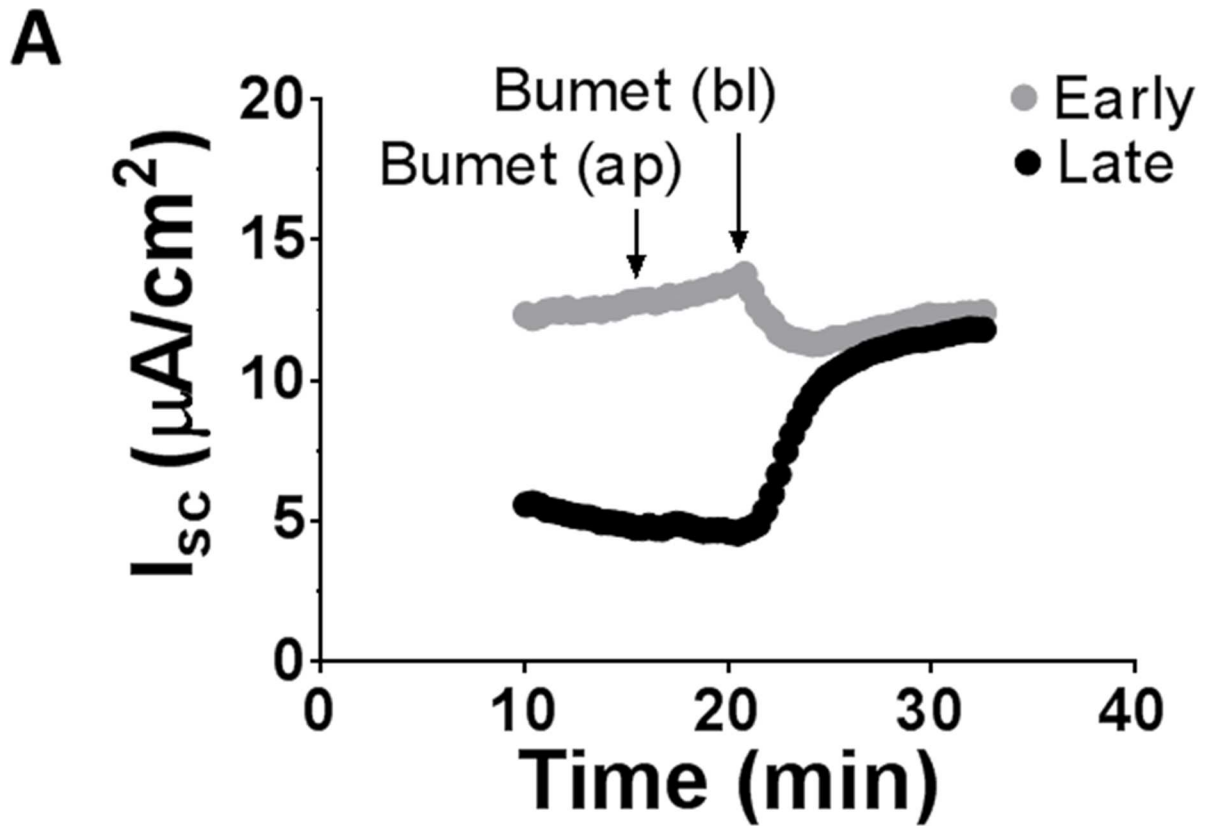
Fig 1. I_{sc} responses to apical and basolateral bumetanide in early and late distal colon of rats. Measurements were made in normal Ringer solution. Note that while apical bumetanide (100 µM) had no effect on either colonic segment, basolateral bumetanide (100 µM) induced two opposite I_{sc} responses: inhibitory in early but stimulatory in late distal colon. ap, apical; bl, basolateral. ** P<0.01 *vs.* absence of bumetanide using paired *t* test. N = 10.

significant I_{sc} increase, rather than the anticipated I_{sc} decrease. Thus, it appears that an unusual electrogenic ion transport mechanism is present in late distal colon.

The stimulatory $I_{sc}^{Bumetanide}$ colocalizes with ENaC-mediated electrogenic Na⁺ absorptive I_{sc} and K⁺ secretory I_{sc} but does not depend on their activities

Apart from actively secreting Cl⁻, the distal colon, particularly the late distal, also actively absorbs Na⁺ and secretes K⁺. It is, therefore, possible that the stimulatory $I_{sc}^{Bumetanide}$ noted in late distal colon might be a Na⁺ absorptive current, a K⁺ secretory current, or both. NKCC1 mediates the influx of Na⁺, K⁺, and 2Cl⁻, utilizing the inward gradient for Na⁺ for the uphill transport of two Cl⁻. Thus, inhibition of NKCC1 by bumetanide not only decreases Cl⁻ secretion, but may also reduce cellular Na⁺ and K⁺; the resultant reduction of cellular Na⁺ and K⁺ may result in stimulation of ENaC and blockage of spontaneous K⁺ secretion, leading to an increase in I_{sc}. To explore these possibilities, we examined I_{sc} responses to basolateral bumetanide following inhibition of the activities of apical ENaC and K⁺ secretion by amiloride and barium, respectively (Fig 2). Indeed, under present experimental conditions electrogenic Na⁺ absorption and K⁺ secretion were present in the late distal colon, as evidenced by amiloride-induced decrease of I_{sc} and barium-induced increase of I_{sc} (Fig 2A). However, prior inhibition of these ion transporters did not significantly alter the bumetanide-induced I_{sc} responses, neither in early nor late distal colon (Fig 2A; quantitative summary in Fig 2B), thus excluding the contribution of Na⁺ absorptive or K⁺ secretory current.

Since the lack of effect of amiloride was not anticipated, a 10x higher dose (100 µM) amiloride was used to be certain that inhibition of ENaC activity was complete. We also tested the effect of benzamil, a more potent ENaC inhibitor. The I_{sc} responses to bumetanide remained unaltered with either inhibitor (Table 2). Since the dose of 100 µM amiloride used also inhibits Na⁺/H⁺ exchange, the lack of effect of the latter suggests that Na⁺/H⁺ exchange is not also contributing.

Bumetanide stimulation of I_{sc} requires Cl⁻ and is inhibited by Cl⁻ channel inhibitors

The question then arises of whether the positive I_{sc} induced by bumetanide is a Cl⁻ current. To address this, Cl⁻ ion substitution experiments were performed (Fig 3). In these experiments, Cl⁻ was replaced by isethionate. As a control, the effects without Na⁺ were also examined. In

Table 1. Basal bioelectric parameters in rat early and late distal colon.

	Early distal colon	Late distal colon
I_{sc}, µA/cm^2	65.0 ± 12.7 (10)	24.7 ± 3.3 (10)**
R, Ω.cm^2	70.9 ± 11.6 (10)	122.7 ± 15.3 (10)**
PD, mV	5.8 ± 1.1 (10)	4.5 ± 0.9 (10)

Data shown are means ± SEM (n).

** P<0.01 *vs.* Early distal colon.
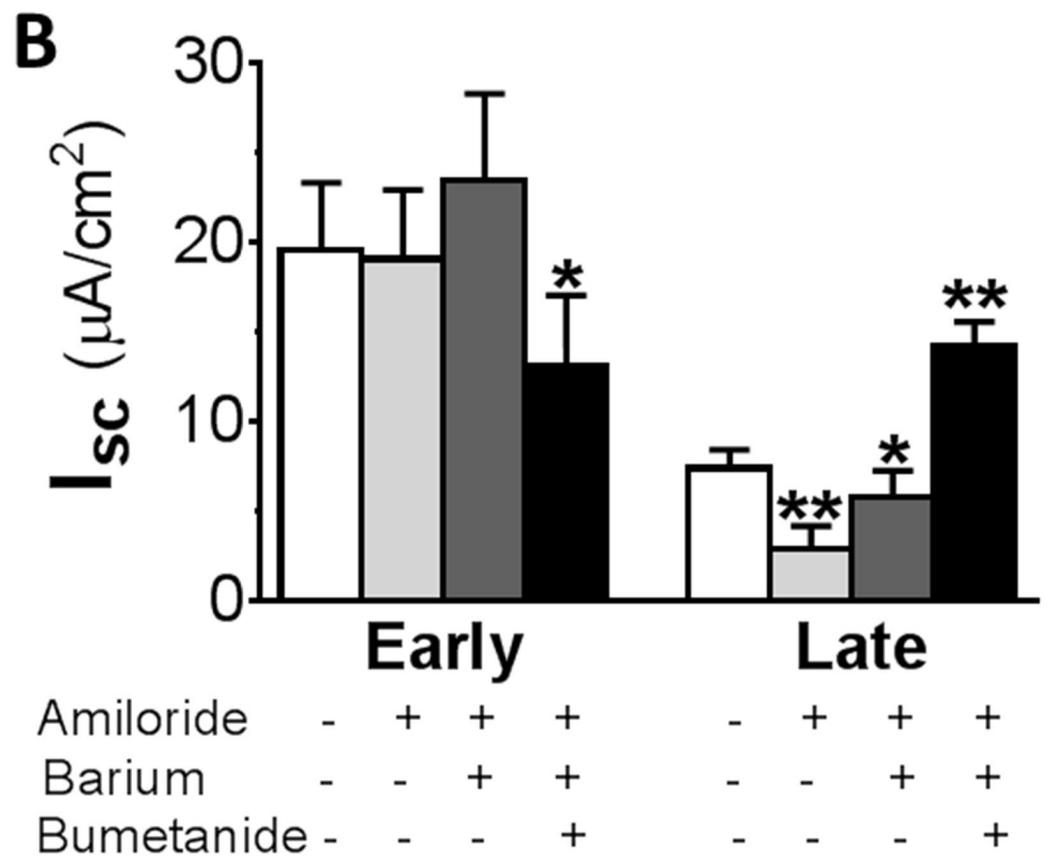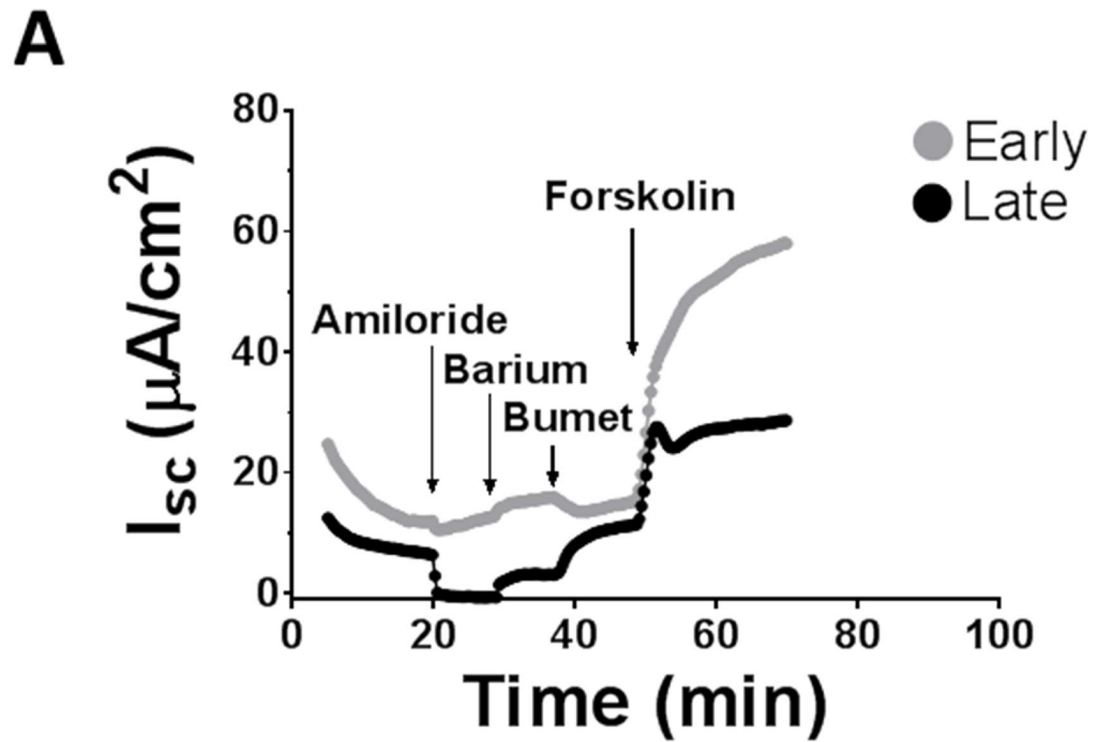
Fig 2. I_{sc} responses to basolateral bumetanide in the presence of amiloride and barium. I_{sc} was measured in normal Ringer solution. Note that amiloride (10 μM, apical) significantly decreased and barium (5 mM, apical) significantly increased I_{sc} in late distal colon. However, these treatments did not alter the subsequent I_{sc} responses to bumetanide (100 μM, basolateral) in either colonic segment. Subsequent addition of forskolin (500 nM, basolateral) caused I_{sc} stimulation in both segments (see text). * P<0.05 and ** P<0.01 *vs.* prior treatment by paired *t* test. N = 10.

doi:10.1371/journal.pone.0171045.g002

the latter case, Na⁺ was replaced by NMDG⁺. In normal Ringer solution, the $\Delta I_{sc}^{Bumetanide}$ was negative or inhibitory in early distal colon and positive or stimulatory in late distal colon. Neither inhibitory nor stimulatory responses by bumetanide were altered when Na⁺ was removed from Ringer solution. In contrast, both responses to bumetanide were completely abolished when Cl⁻ was eliminated from solution, indicating that, like the inhibitory $I_{sc}^{Bumetanide}$, the stimulatory $I_{sc}^{Bumetanide}$ is also a Cl⁻ current.

Considering the current direction opposite to the known Cl⁻ secretory I_{sc} and the current location in the salt absorptive late distal colon, it is possible that this positive $I_{sc}^{Bumetanide}$ is a Cl⁻ absorptive current. Cl⁻ could be entering the cell down its concentration gradient via apical Cl⁻ channels and subsequently be extruded from the basolateral membrane via the bumetanide-sensitive KCl cotransporter (KCC) using the downhill K⁺ gradient provided by the basolateral Na⁺,K⁺-ATPase (see Discussion below). To address this possibility, we examined the effects of Cl⁻ channel inhibitors NPPB [20] and glibenclamide [21, 22].

Fig 4 shows effects of NPPB/glibenclamide on I_{sc} responses to bumetanide. As controls, the effects of NPPB/glibenclamide on subsequent I_{sc} responses to forskolin (a measure of cAMP-activated anion channels) and carbachol (a measure of Ca²⁺-activated anion channels) were also assessed. Consistent with the presence of an active Cl⁻ absorptive conductance in the apical membrane of late distal colonic epithelium, the addition of NPPB/glibenclamide to the apical bath increased I_{sc} in late distal colon (Fig 4A). In contrast, the same pretreatment caused an I_{sc} decrease in early distal colon (Fig 4A), in keeping with inhibition of Cl⁻ secretory conductance in the apical membrane of early distal colonic epithelium. Importantly, following NPPB/glibenclamide pretreatment, while the I_{sc} responses to amiloride remained unchanged, the I_{sc} responses to bumetanide was significantly attenuated or abolished (Fig 4A & 4B). NPPB/glibenclamide pretreatment also significantly attenuated the I_{sc} responses to forskolin [compare Fig 4A (presence of inhibitors) with Fig 2A (absence of inhibitors)] but not to carbachol (see Fig 4A). Similar effects were observed with GlyH 101 but not CFTR(inh)-172. This suggests the possible involvement of Cl⁻ conductance in Cl⁻ absorption by late distal colon.

## Effect of bumetanide on transepithelial conductance in distal colon

To provide further evidence that a channel conductance is implicated in Cl⁻ absorptive I_{sc} in late distal colon, effects on transepithelial conductance (G_T) were examined (Fig 5). If a

Table 2. Effects of amiloride and benzamil on $\Delta I_{sc}^{Amiloride}$ and $\Delta I_{sc}^{Bumetanide}$ in rat early and late distal colon*.

	$\Delta I_{sc}^{Amiloride}$, μA/cm²		$\Delta I_{sc}^{Bumetanide}$, μA/cm²	
	Early distal colon	Late distal colon	Early distal colon	Late distal colon
None			-17.4 ± 3.1 (10)	22.3 ± 3.8 (10)
Amiloride (10μM)	-1.5 ± 0.7 (10)	-6.2 ± 6.8 (10)	-26.2 ± 5.1 (10)ns	27.2 ± 6.4 (10)ns
Amiloride (100μM)	-2.2 ± 0.8 (4)NS	-10.0 ± 7.3 (4)NS	-17.0 ± 2.0 (4)ns	37.0 ± 11.0 (4)ns
Benzamil (5μM)	-1.8 ± 0.8 (4)NS	-6.3 ± 3.8 (4)NS	-12.0 ± 4.0 (4)ns	33.0 ± 2.0 (4)ns

* $\Delta I_{sc}^{Amiloride}$ refers to induced ΔI_{sc} before and after indicated drug treatment. Data shown are means ± SEM (n). ns P>0.05 *vs.* None. NS P>0.05 *vs.* Amiloride (10μM).

doi:10.1371/journal.pone.0171045.t002
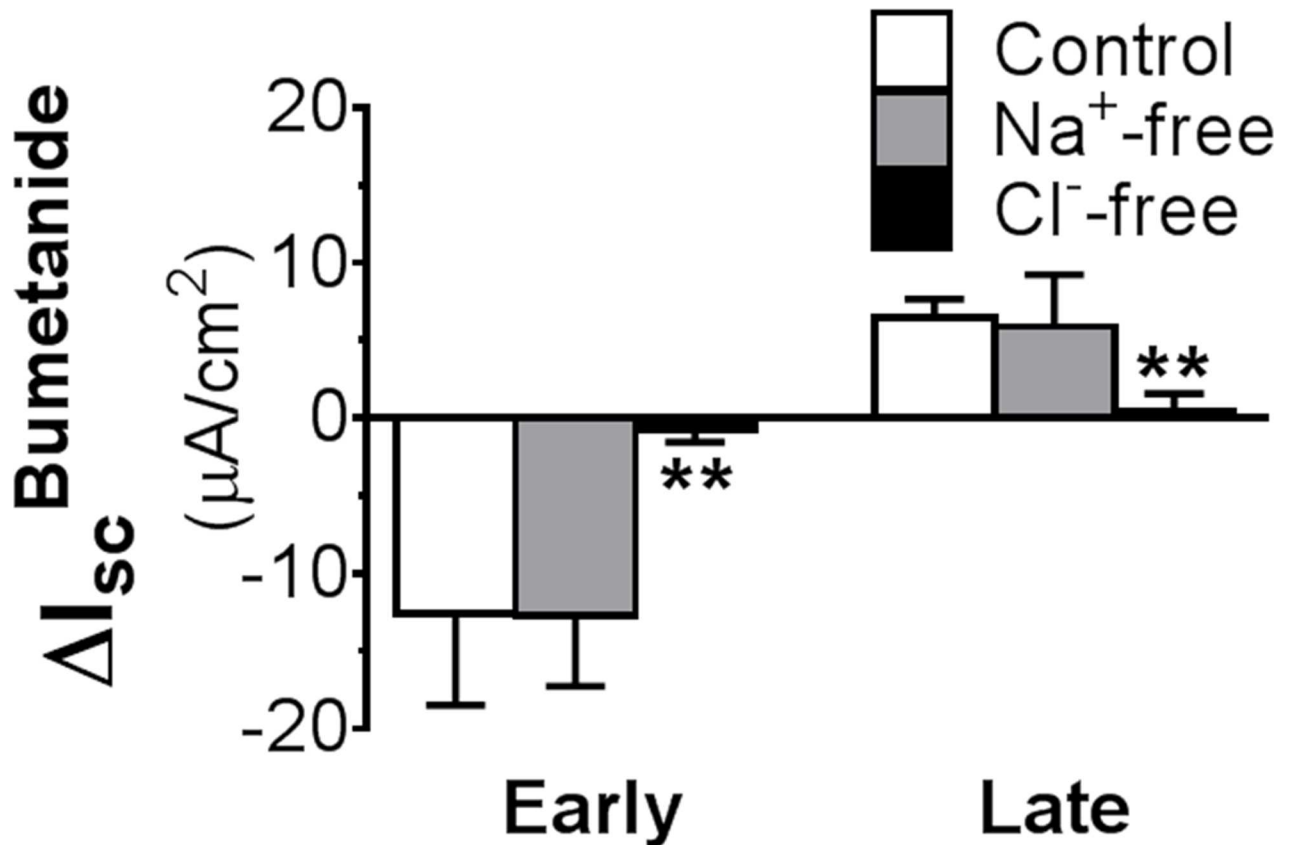
Fig 3. Effects of ion substitution on changes in I_{sc} responses to basolateral bumetanide (100 µM) in early vs. late distal colon. Note the two opposing $\Delta I_{sc}^{Bumetanide}$: negative or inhibitory in early distal colon and positive or stimulatory in late distal colon. While Na$^+$ substitution caused no significant change in the I_{sc} response in either colonic segment, removal of Cl$^-$ from media abolished the I_{sc} responses in both segments. ** P<0.01 vs. control. N = 8–12.

doi:10.1371/journal.pone.0171045.g003

channel conductance is involved in this transport process, bumetanide treatment should inhibit this channel activity and decrease G_T. As illustrated in Fig 5A, bumetanide decreased G_T, not only in early but also in late distal colon. The G_T decrease by bumetanide was significantly more pronounced in late than early distal colon (Fig 5B).

As a control, the effect of forskolin on G_T was also examined (Fig 5A & 5C). Forskolin increased G_T. In contrast to the pattern induced by bumetanide, the G_T increase by forskolin was more pronounced in early than late distal colon. The forskolin-induced increases in G_T along early and late distal colon are very similar to those found for forskolin-induced I_{sc} (see Fig 2A) and CFTR mRNA (see Fig 6 below), consistent with the known forskolin stimulating effect on CFTR conductance [2].

Together, the results indicate that a transepithelial conductance is inhibited in late distal colon by bumetanide concurrently with transepithelial I_{sc} activation. Based on this and other findings, we concluded that an electrogenic Cl⁻ absorptive mechanism is present in late distal colon. This mechanism involves a NPPB/glibenclamide-sensitive Cl⁻ conductance (likely a CFTR-like Cl⁻ channel/transporter) in the apical membrane, which mediates Cl⁻ entry, and a bumetanide-sensitive Cl⁻ absorbing mechanism (likely a KCl cotransporter) in the basolateral membrane, which mediates Cl⁻ exit.

A

B
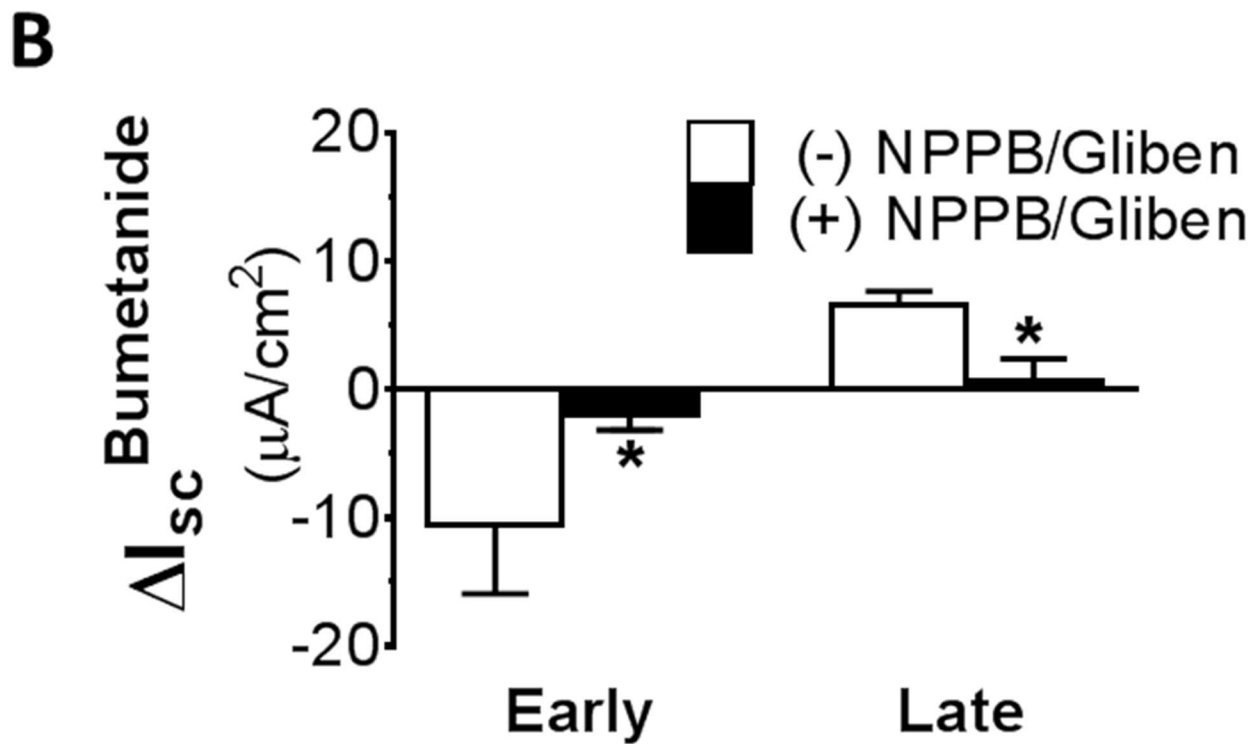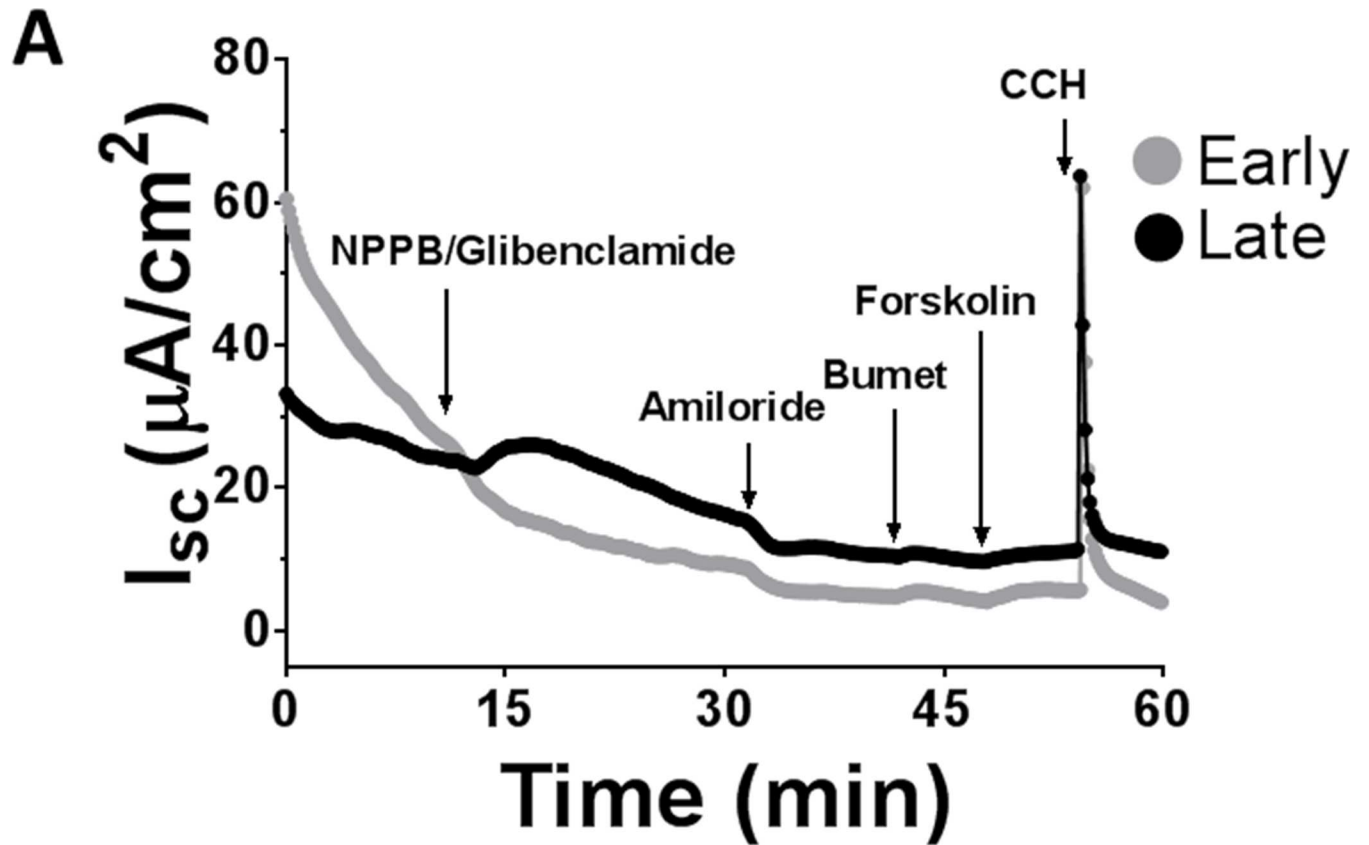
Fig 4. Effects of Cl⁻ channel inhibitors on I_{sc} responses to basolateral bumetanide in early and late distal colon of rats. Measurements were made in normal Ringer solution. Note that pretreatment with NPPB (100 μM, apical) and glibenclamide (300 μM, apical) significantly attenuated I_{sc} responses to bumetanide (100 μM, basolateral) and forskolin (500 nM, basolateral), but not to amiloride (10 μM, apical) or carbachol (CCH, 100 μM, basolateral). **P<0.05 *vs.* (-) NPPB/Glibenclamide. N = 5.

doi:10.1371/journal.pone.0171045.g004

Expression of ion transporter in the distal colon

To further characterize this electrogenic Cl⁻ absorptive I_{sc}, RNA sequencing analysis was performed on gene transcripts of major ion transporters in rat distal colon (Table 3 & Fig 6). Consistent with the notion that late distal colon differs from early distal colon in salt transport, it was found that transporters associated with salt absorption were expressed in a pattern
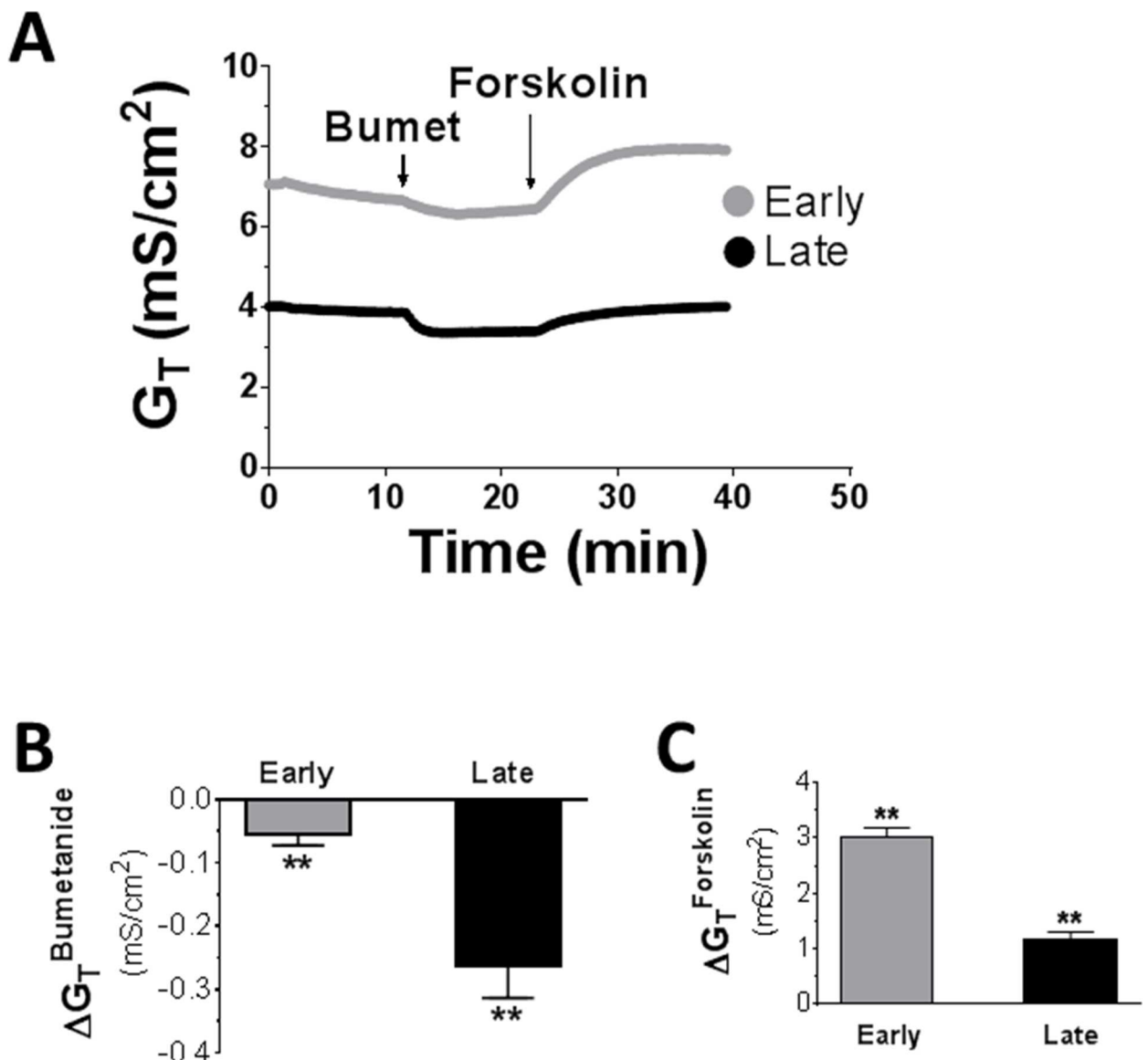
Fig 5. Transepithelial conductance (G_T) responses to bumetanide (100 μM, basolateral) and forskolin (500 nM, basolateral) in early and late distal colon of rats. The experiments were performed in normal Ringer solution. ** P<0.01 *vs.* prior drug treatment. N = 10.

doi:10.1371/journal.pone.0171045.g005

Fig 6. Differential expression of gene transcripts in late distal colon of rats relative to early distal colon. Positive values indicate more abundant transcripts of indexed gene in late than in early distal colon whereas negative values indicate less abundant transcripts of indexed gene in late than in early distal colon. * P<0.05 *vs.* early distal colon.

opposite to transporters responsible for salt secretion; that is, a greater level of expression was noted for ENaC, NCC, H$^+$,K$^+$-ATPase and CLC in late distal colon when compared with early distal colon segment. On the contrary, a greater level of expression for NKCC1, SBC1, AE2 and CFTR was noted in early distal colon when compared with late distal colon. Interestingly, a similar reciprocal expression pattern was also noted for DRA *vs.* NHE3 in late *vs.* early distal

Table 3. Differential expression of gene transcripts in rat distal colon.

Transporter	Gene	Late	Early	Fold change (late/early)
ENaC-alpha	Scnn1A	251.96	152.597	1.651146*
ENaC-beta	Scnn1B	15.9184	7.42909	2.142712*
ENaC-gamma	Scnn1G	1.77275	0.43038	4.119034*
Na,K-ATPase-alpha1	atp1a1	849.136	974.578	-1.14773
Na,K-ATPase-alpha2	atp1a2	0.116211	0.545423	-4.69339*
Na,K-ATPase-alpha3	atp1a3	0.031001	0.112315	-3.62297*
Na,K-ATPase-beta1	atp1b1	2230.14	1901.33	1.172937
Na,K-ATPase-beta2	atp1b2	0.278041	0.621188	-2.23416*
Na,K-ATPase-beta3	atp1b3	13.679	15.5672	-1.13804
Na,K-ATPase-gamma	fxyd2	2.89002	25.9343	-8.97374*
Na/H exchanger-1	SLC9A1	63.3886	60.385	1.049741
Na/H exchanger-2	SLC9A2	174.178	136.345	1.27748
Na/H exchanger-3	SLC9A3	46.8226	328.108	-7.00747*
NHERF-1	Slc9a3r1	420.365	342.149	1.228602
NHERF-2	Slc9a3r2	5.00395	9.30693	-1.85992*
Na/H exchanger-5	SLC9A5	0.896523	1.13444	-1.26538
Na/H exchanger-6	Slc9a6	8.55022	7.7633	1.101364
Na/H exchanger-8	Slc9a8	18.4983	19.1032	-1.0327
NKCC2	Slc12a1	0	0	
NKCC1	Slc12a2	62.0267	109.889	-1.77164*
NCC	Slc12a3	8.17396	3.357	2.4349*
KCC1	Slc12a4	2.27527	2.63623	-1.15864
KCC2	Slc12a5	0.032339	0.029925	1.080664
KCC3	Slc12a6	16.8354	14.2482	1.181581
	SLC12a7	47.3722	42.1302	1.124424
CCC9	Slc12a8	32.1545	43.3327	-1.34764
CCC6/CIP1	Slc12a9	27.1636	26.4798	1.025823
	Slc26a1	0.348735	0.475976	-1.36486
	Slc26a2	96.8234	93.6515	1.033869
DRA	Slc26a3	1079.2	673.093	1.603345*
Pendrin	Slc26a4	0	0	
Prestin	Slc26a5	0	0	
PAT1	Slc26a6	6.01403	4.71441	1.27567

* P<0.05 *vs.* early distal colon. Positive values indicate more abundant transcripts of indexed gene in late than in early distal colon whereas negative values indicate less abundant transcripts of indexed gene in late than in early distal colon.

colonic segments. This segregated pattern contrasts with the coupled DRA/NHE3 expression proposed for electroneutral NaCl absorption in the colon [2]. Unlike the transcripts for transporters specific for salt absorption and secretion, the transcripts for Na^+,K^+-ATPase (NKA), which is required for both salt absorption and secretion, remained stable in the distal colon. In disagreement with a previous report [23], NKCC2 transcripts were not detected in either colonic segment.

Of note, while transcripts of NKCC1 were found to be differentially expressed within the distal colon and may explain the difference in Cl⁻ secretory I_{sc}, such differential distribution was not detected for KCC1 mRNAs. To assess if differential distribution for KCC1 exists at the protein level, Western blot analyses using a specific anti-KCC1 antibody were performed (Fig 7). Approximately two-fold higher KCC1 protein was detected in late than early distal colon.

Together, the results indicate that the segmental heterogeneity in I_{sc} response to bumetanide may represent different patterns of distribution of the two bumetanide-sensitive cation chloride cotransporters, NKCC1 and KCC1. Although NKCC1 and KCC1 both mediate secondary active transport of Cl⁻ through the tight coupling to movement of a cation, they are driven by different electrochemical gradients generated by NKA and therefore result in different outcomes in Cl⁻ homeostasis. Whereas NKCC1 mediates Na^+ gradient-dependent inward transport of Cl⁻, which increases $[Cl^-]_i$ leading to Cl⁻ secretion, KCC1 mediates K^+ gradient-dependent outward movement of Cl⁻, which decreases $[Cl^-]_i$ resulting in Cl⁻ absorption. Accordingly, the direction of Cl⁻ transport is determined by the relative expression of these two transporters in segments of distal colon. Since the early distal colon expresses more NKCC1 than KCC1, Cl⁻ secretion observed, whereas the late distal colon expresses more KCC1 than NKCC1 and thus is Cl⁻ absorptive.

Effects of salt depletion and repletion

To understand the physiological role this active Cl⁻ absorptive mechanism may play in the salt-sensitive distal colon, experiments that altered NaCl in the diet were performed. In these experiments, animals were subjected to either low or high salt treatment (via diet or drink) for 1 week before colonic I_{sc} responses to bumetanide were determined (Fig 8). As positive control, colonic I_{sc} responses to low dose amiloride were also assessed (Table 4). While no significant changes were found in early distal colon (Fig 8), in late distal colon, decreasing NaCl intake significantly increased the Cl⁻ absorptive I_{sc}, whereas increasing NaCl intake significantly decreased it (Fig 8). Similar increases and decreases to low and high salt diets, respectively, were also noted for amiloride-sensitive ENaC current (Table 4). These data established that an active Cl⁻ absorptive mechanism is present in late distal colon in parallel with ENaC, and that it is actively involved in NaCl absorption when salt is in deficit.

Discussion

Unlike other extracellular milieu, the lumen of the colon is home to hundreds of trillions of bacteria. There, as high as 120 mM of short-chain fatty acids (SCFA) are normally present due to bacterial fermentation of undigested carbohydrates [3, 4]. Accordingly, in the lumen of the colon, the major anions are SCFA; other anions, such as Cl⁻, are low [5]. For passive Cl⁻ absorption to occur at low $[Cl^-]_L$, apical membrane potential (Ψ_a) must depolarize markedly to maintain the driving force for Cl⁻ entry into the cell across the apical membrane. Alternatively, intracellular Cl⁻ concentration ($[Cl^-]_i$) must fall appreciably. In the distal colon, while Ψ_a depolarizes due to ENaC-mediated electrogenic Na^+ absorption, it also hyperpolarizes due to spontaneous electrogenic K^+ secretion. Furthermore, unlike exclusive absorptive epithelia (e.g., sweat duct), colonic epithelia have a more complex task of providing both absorption
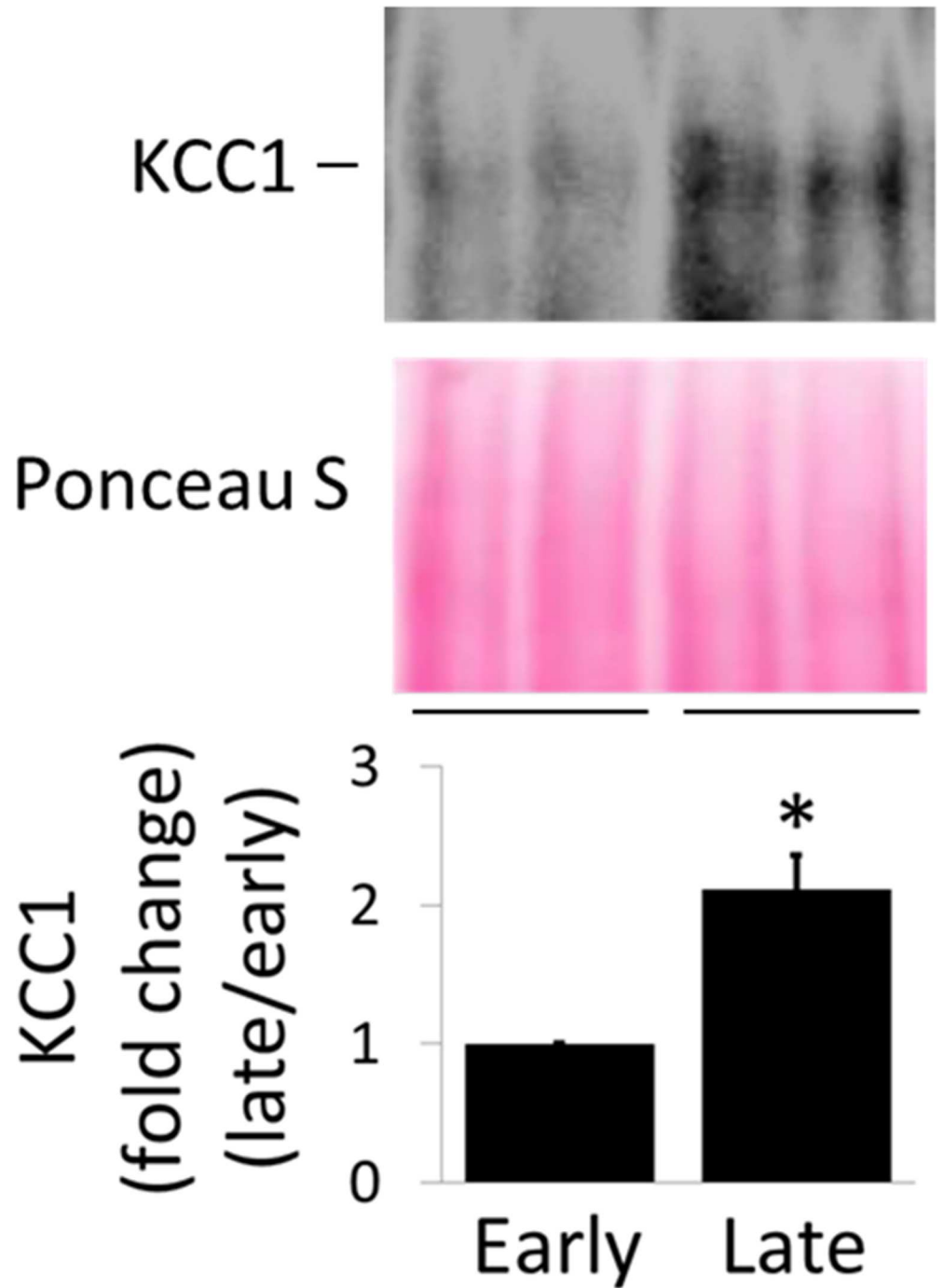
Fig 7. Differential expression of KCC1 protein in late distal colon of rats relative to early distal colon. **Upper panel**, Western blots of KCC1; **Middle panel**, Ponceau S staining; **Lower panel**, The Western blots were quantified and normalized to ponceau S staining. The y-axis represents relative values (changes in fold) with respect to the values of early distal colon. * P<0.05 *vs.* early distal colon. N = 5.

and secretion of Cl⁻, and $[Cl^-]_i$ may or may not fall in this tissue due to the presence of Cl⁻ entry into the cell from the basolateral NKCC1 [2] or Cl⁻/ HCO_3^- exchanger [13]. Thus, it is not entirely clear whether the changes in Ψ_a and $[Cl^-]_i$ are sufficient to maintain the driving
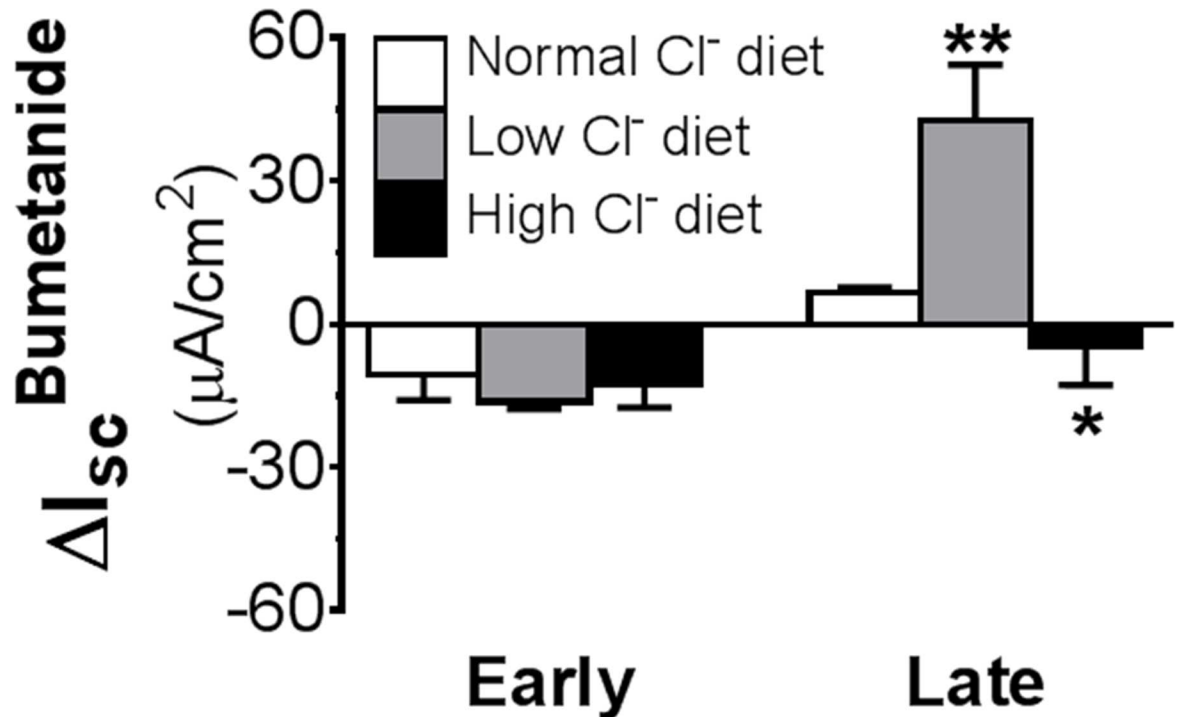
Fig 8. Effects of dietary Cl⁻ depletion and repletion on I_{sc} responses to basolateral bumetanide in early and late distal colon. Note that dietary Cl⁻ depletion enhanced whereas dietary Cl⁻ repletion reduced the positive I_{sc} induced by basolateral bumetanide (100 μM) in late distal colon but had no effect on the induced negative I_{sc} in early distal colon. * P<0.05 and ** P<0.01 *vs.* normal Cl⁻ diet. N = 6–10.

doi:10.1371/journal.pone.0171045.g008

force for Cl⁻ influx from the lumen, requisite for passive Cl⁻ absorption to occur in a low $[Cl^-]_L$ situation. It is likely that an alternative active mechanism for Cl⁻ absorption is present in the distal colon, particularly in the late distal colon where, due to reabsorption, $[Cl^-]_L$ is the lowest [5].

In these present studies, we presented evidence that an alternative Cl⁻ absorptive mechanism exists in the late distal colon. This Cl⁻ absorptive mechanism is active and electrogenic; it operates in parallel with ENaC-mediated Na⁺ absorption, but does not depend on ENaC activity, as proposed per current model [2]. Also in support of electrogenic Cl⁻ absorption in this colonic segment is the observation that the late distal colon is tighter than its early counterpart. This is evidenced by higher electrical resistance and lower lumen negative potential difference and I_{sc} (see Table 1). Given its sensitivity to apical NPPB/glibenclamide and basolateral bumetanide, we proposed a transport model for this alternative Cl⁻ absorption process (see Fig 9).

Table 4. $I_{sc}^{Amiloride}$ responses to low and high salt diet treatments in rat distal colon.

	$\Delta I_{sc}^{Amiloride}$, μA/cm²	
	Early distal colon	**Late distal colon**
Control diet	1.24 ± 0.26 (8)	5.50 ± 1.17 (8)**
Low salt diet	2.92 ± 1.29 (6)#	28.08 ± 6.61 (6)**##
High salt diet	0.12 ± 0.02 (3)##	0.77 ± 0.39 (3)*#

Data shown are means ± SEM (n).

* P<0.05 and ** P<0.01 *vs.* Early distal colon.

P<0.01 and #P<0.05 *vs.* control.

doi:10.1371/journal.pone.0171045.t004
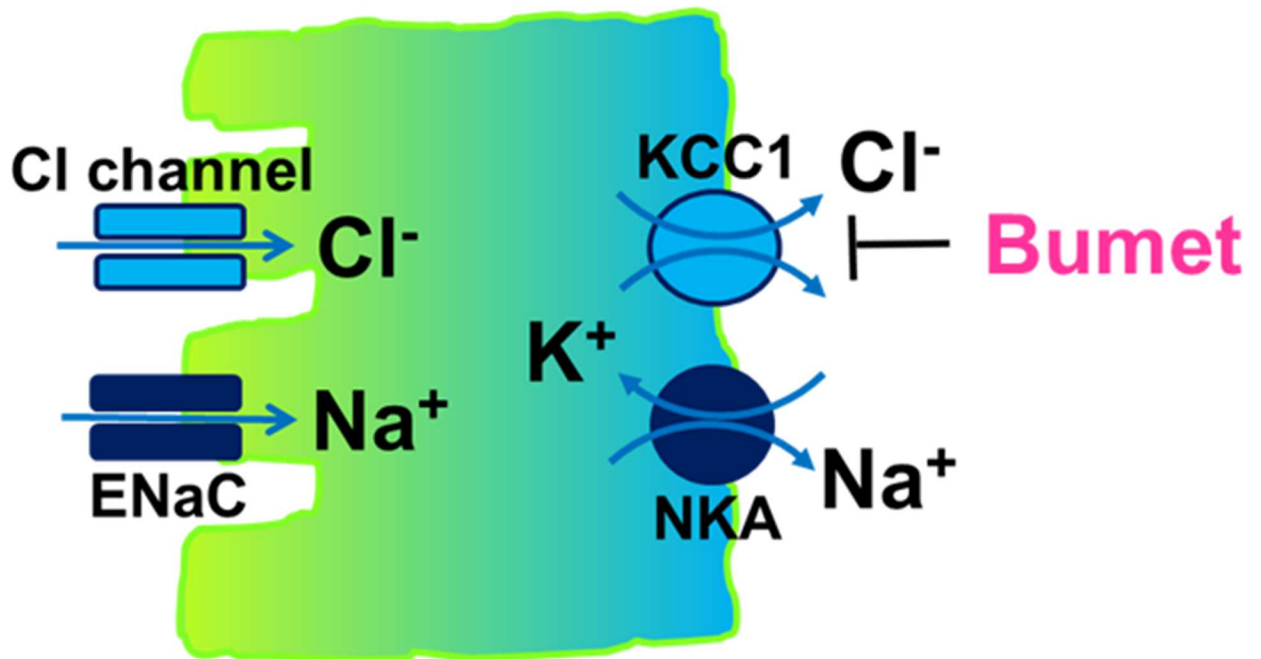
Fig 9. Transport model for electrogenic Cl⁻ absorption in surface cell of late distal colonic epithelium. Cl⁻ enters via a Cl⁻ channel conductance and egresses through a bumetanide-sensitive K⁺-Cl⁻ cotransporter. K⁺ is recycled uphill into the cell by Na⁺,K⁺-ATPase (NKA), while the latter pumps Na⁺ that enters via ENaC against electrochemical gradient out of the cell. Thus, transepithelial Na⁺ and Cl⁻ absorption are both an active process and operate in parallel.

doi:10.1371/journal.pone.0171045.g009

According to this new model, Na^+ and Cl^- move in parallel and are both actively absorbed. The energy that drives Na^+ and Cl^- uptakes is derived from the basolateral Na⁺,K⁺-ATPase (NKA). Through active pumping of Na^+ out of the cell and K^+ into the cell, NKA lowers intracellular Na^+ concentration ($[Na^+]_i$) and elevates intracellular K^+ concentration ($[K^+]_i$), generating two chemical gradients across cell membrane: the gradient for Na^+ and the gradient for K^+. Whereas the gradient for Na^+ enables apical ENaC to move Na^+ from the lumen into the cell, the gradient for K^+ provides the driving force for active uptake of Cl^- via the secondary active basolateral bumetanide-sensitive KCl cotransporter [24] (likely KCC1 [25]), which extrudes one K^+ with one Cl^- from the cell to the blood, and so lowers $[Cl^-]_i$; the apical NPPB/glibenclamide-sensitive Cl^- conductance (likely a Cl^- channel/transporter) subsequently moves Cl^- from the lumen into the cell.

It is worth noting, however, that the model described in Fig 9 is the simplest one. It describes the basic components required for active uptake of Cl^- in this part of the colon. Other transporters may be involved to facilitate this transport process. These may include: 1) basolateral K^+ channel. This K^+ channel may participate in the fine-tuning of the activity of KCC1 through adjusting $[K^+]_i$; 2) basolateral Cl^-/HCO_3^- exchange. There are reports that this anion exchange may contribute to Cl^- secretion [13] and Cl^- absorption [2]; 3) apical Na⁺-Cl⁻ cotransporter (NCC) [26]. NCC transcript was expressed in late distal colonic mucosa (see Table 3 and Fig 6). NCC is likely present at the apical membrane of distal colonic epithelial cells, facilitating Cl^- entry, particularly when $[Cl^-]_L$ is low; 4) apical DRA [27]. As a member of the SLC26 family, this Cl^-/HCO_3^- exchanger is reported to have concurrent conductive Cl^- activity [28]. Thus, it may help provide an additional pathway or source of energy to take up Cl^- from the lumen when $[Cl^-]_L$ is low through using the gradient of HCO_3^- generated internally through the hydration of CO_2 by carbonic anhydrase [29–31].

In sweat duct, frog skin, and other high-resistance (400 ohm.cm^2 or higher) epithelia, Cl$^-$ absorption is achieved primarily through coupling to active Na$^+$ absorption [10, 32]. In these non-leaking epithelia, a separate active mechanism for Cl$^-$ absorption is biophysically unnecessary. Compared to these tight epithelia, the resistance of colon epithelium is much lower (150 ohm.cm^2 or lower) (see Table 1; also refs [11, 15]). While being leaky may confer to this colonic epithelium the ability to perform other beneficial functions such as absorbing luminal nutrients and monitoring luminal microbiota, it also makes it difficult to simply couple Cl$^-$ absorption passively to Na$^+$ absorption. To achieve the goal of regulating salt homeostasis in this physiologically important epithelium, a parallel active Cl$^-$ absorption is necessary. This active Cl$^-$ absorption differs from the transcellular Cl$^-$ absorption that couples to ENaC in the sweat duct. It also differs from the Cl$^-$ absorption that occurs via a paracellular Cl$^-$ shunt in leaky proximal tubule and other intestinal epithelia. This active Cl$^-$ flux runs in parallel with ENaC (see Fig 9). Thus, the presence of this active Cl$^-$ transport would best fulfill the function of the colon by this epithelium.

Like ENaC, this active Cl$^-$ absorption is regulated in accordance with the salt status of the body. Consequently, when NaCl is in excess, e.g., when dietary salt intake is increased, it is down regulated (see Fig 8). In contrast, when NaCl is in deficit (i.e., when dietary salt intake is decreased or in pathological situations such as in diarrhea or diuresis in which high salt loss occurs), it is up regulated (see Fig 8). In response to salt depletion, aldosterone is secreted [33], which then stimulates electrogenic Na$^+$ absorption in the distal colon as well as the distal nephron via up regulation of ENaC, NKA, and their regulators such as SGK and CHIF [33]. Whether aldosterone stimulates parallel electrogenic Cl$^-$ absorption is unknown; also uncertain is whether this occurs via the up-regulation of CFTR in the ENaC-expressing absorbing surface epithelium of the distal colon/nephron. In addition to aldosterone, the extracellular calcium-sensing receptor (CaSR) is another key receptor mechanism that regulates homeostasis of salt transport, particularly in the gut, where CaSR coordinates monovalent and divalent ion homeostasis [34–36]. Increases of luminal as well as serosal [Ca^{2+}] and CaSR activity decrease electrogenic Cl$^-$ secretion [15, 18, 37, 38]; they also increase electroneutral NaCl absorption [11, 38]. The goal is to ensure, along with CaSR-mediated regulation in parathyroid and kidney, that extracellular [Ca^{2+}] is stable without significant elevations. Whether CaSR increases electrogenic Na$^+$ and Cl$^-$ absorption in this highly regulated late distal colon remains to be determined.

Previous studies have shown significant segmental heterogeneity between the proximal and distal colon in terms of ion transport function and sensitivity to aldosterone stimulation. For example, basal K$^+$ movement is secretory (via apical K$^+$ channel conductance [39]) in the proximal colon but is absorptive (via apical H$^+$,K$^+$-ATPase [40]) in the distal colon. Their responses to aldosterone stimulation and dietary K$^+$ loading also differ, with enhancing K$^+$ secretion in the proximal colon versus converting K$^+$ movement from absorption to secretion in the distal colon [41]. Similar differences are also seen in Na$^+$ transport. Without aldosterone the basal Na$^+$ absorption is electroneutral (via NHE3) in the proximal colon and is electroneutral (via NHE3) and electrogenic (via ENaC) in the distal colon [2, 42]. Aldosterone stimulation enhances NHE3-mediated Na$^+$ transport in the proximal colon [43], but causes a flip of Na$^+$ transport from NHE3 to ENaC in the distal colon [44]. Consistent with this aldosterone flip, our functional studies in the distal colon revealed a significant increase in ENaC current (2-fold increase in early distal colon and 5-fold increase in late distal colon, P<0.01) in response to dietary Na$^+$ depletion and a significant decrease (10-fold decrease in the early distal colon and 7-fold decrease in the late distal colon, P<0.01) in response to dietary Na$^+$ repletion (Table 4). It would be interesting to know if these dietary treatments cause inverse changes in NHE3 function.

In the present study, we show that a discrepancy also exists within the distal colon between the early and the late distal colon segments. We found that while the early distal colon was

predominantly salt secretory, the late distal colon was primarily salt absorptive. Accordingly, inversed profiles of ion transporters for secretion and for absorption were seen, with CFTR, NKCC1 and SBC1 being more abundant in the early distal colon than the late distal colon, and ENaC and KCC1 being prominent in the late distal colon and negligible in the early distal colon (see Table 3, Fig 6 and Fig 7). Consistent with this arrangement, we found that, although both currents are present in both segments, the Cl⁻ secretory I_{sc}, which, in current direction, is inhibitory by bumetanide, was primarily localized to the salt secretory early distal colon, whereas the Cl⁻-absorptive I_{sc}, which, in current direction, is stimulatory by bumetanide, was primarily present in the salt absorptive late distal colon (see Fig 1). The results from our physiological study have confirmed this functional arrangement. Accordingly, secretagogues (e.g., forskolin) stimulate salt secretion primarily in the early distal colon (see Fig 2), whereas aldosterone/low salt diet intake stimulates salt absorption mainly in the late distal colon (see Fig 8). Thus, the cycling of fluid and electrolytes through segregated secretion and absorption appears to be a common theme in the mammalian intestine.

In summary, our present studies demonstrate the following: 1) rat distal colonic epithelium is able to both actively secrete and absorb Cl⁻, with secretion primarily occurring in ENaC-absent early distal colon and absorption predominantly in ENaC-expressing late distal colon; 2) active Cl⁻ absorption in the late distal colon is increased by dietary Cl⁻ (salt) depletion and decreased by dietary Cl⁻ (salt) repletion; and 3) active Cl⁻ absorption occurs through transcellular transport that involves an apical NPPB/glibenclamide-sensitive Cl⁻ conductance and a basolateral bumetanide-sensitive K^+-Cl⁻ cotransporter. We conclude that an electrogenic Cl⁻ extrusion mechanism exists and operates in parallel with the electrogenic ENaC in the distal colon (and probably in nephron as well) where the final control of NaCl absorption occurs before effluents are discharged from the body.

Acknowledgments

Author contributions

Conceptualization: SXC.

Formal analysis: LT XF SXC.

Funding acquisition: SAR SXC.

Investigation: LT XF SPW CYC SXC.

Methodology: LT XF SXC.

Project administration: LT SXC.

Resources: XF.

Supervision: SXC.

Validation: SXC.

Visualization: LT XF CYC SXC.

Writing – original draft: LT CYC SXC.

Writing – review & editing: CYC HJB SXC.

References

1. Welsh MJ, Smith PL, Fromm M, Frizzell RA. Crypts are the site of intestinal fluid and electrolyte secretion. Science. 1982; 218(4578):1219–21. PMID: 6293054

2. Kunzelmann K, Mall M. Electrolyte transport in the mammalian colon: mechanisms and implications for disease. Physiological reviews. 2002; 82(1):245–89. doi: 10.1152/physrev.00026.2001 PMID: 11773614

3. Hammer HF, Santa Ana CA, Schiller LR, Fordtran JS. Studies of osmotic diarrhea induced in normal subjects by ingestion of polyethylen glycol and lactulose. The Journal of clinical investigation. 1989; 84 (4):1056–62. doi: 10.1172/JCI114267 PMID: 2794043

4. Binder HJ. Role of colonic short-chain fatty acid transport in diarrhea. Annu Rev Physiol. 2010; 72:297–313. doi: 10.1146/annurev-physiol-021909-135817 PMID: 20148677

5. Talbot C, Lytle C. Segregation of Na/H exchanger-3 and Cl/HCO3 exchanger SLC26A3(DRA) in rodent cecum and colon. American journal of physiology Gastrointestinal and liver physiology. 2010; 299(2): G358–67. doi: 10.1152/ajpgi.00151.2010 PMID: 20466943

6. Wills NK. Apical membrane potassium and chloride permeabilities in surface cells of rabbit descending colon epithelium. The Journal of physiology. 1985; 358:433–45. PubMed Central PMCID: PMC1193351. PMID: 2580086

7. Dorge A, Beck FX, Rechkemmer G. Cellular site of active K absorption in the guinea-pig distal colonic epithelium. Pflugers Archiv: European journal of physiology. 1998; 436(2):280–8. doi: 10.1007/s004240050633 PMID: 9594029

8. Catalan M, Niemeyer MI, Cid LP, Sepulveda FV. Basolateral ClC-2 chloride channels in surface colon epithelium: regulation by a direct effect of intracellular chloride. Gastroenterology. 2004; 126(4):1104–14. PMID: 15057749

9. Jakab RL, Collaco AM, Ameen NA. Physiological relevance of cell-specific distribution patterns of CFTR, NKCC1, NBCe1, and NHE3 along the crypt-villus axis in the intestine. American journal of physiology Gastrointestinal and liver physiology. 2011; 300(1):G82–98. PubMed Central PMCID: PMC3025502. doi: 10.1152/ajpgi.00245.2010 PMID: 21030607

10. Ussing HH, Zerahn K. Active transport of sodium as the source of electric current in the short-circuited isolated frog skin. Acta physiologica Scandinavica. 1951; 23(2–3):110–27. doi: 10.1111/j.1748-1716.1951.tb00800.x PMID: 14868510

11. Tang L, Peng M, Liu L, Chang W, Binder HJ, Cheng SX. Calcium-Sensing Receptor Stimulates Cl— and SCFA-dependent but Inhibits cAMP-dependent HCO3- Secretion in Colon. The American journal of physiology. 2015; 308(10):G874–83.

12. Haas M, McManus TJ. Bumetanide inhibits (Na/K /2Cl) co-transport at a chloride site. The American journal of physiology. 1983; 245(3):C235–40. PMID: 6614157

13. Schultheiss G, Horger S, Diener M. The bumetanide-resistant part of forskolin-induced anion secretion in rat colon. Acta physiologica Scandinavica. 1998; 164(2):219–28. PMID: 9805109

14. Ecke D, Bleich M, Greger R. The amiloride inhibitable Na+ conductance of rat colonic crypt cells is suppressed by forskolin. Pflugers Archiv: European journal of physiology. 1996; 431(6):984–6. PMID: 8927519

15. Cheng SX. Calcium-sensing receptor inhibits secretagogue-induced electrolyte secretion by intestine via the enteric nervous system. The American journal of physiology. 2012; 303(1):G60–G70.

16. Fang X, Poulsen RR, Wang-Hu J, Shi O, Calvo NS, Simmons CS, et al. Knockdown of DNA methyltransferase 3a alters gene expression and inhibits function of embryonic cardiomyocytes. FASEB journal: official publication of the Federation of American Societies for Experimental Biology. 2016.

17. Trapnell C, Roberts A, Goff L, Pertea G, Kim D, Kelley DR, et al. Differential gene and transcript expression analysis of RNA-seq experiments with TopHat and Cufflinks. Nature protocols. 2012; 7(3):562–78. PubMed Central PMCID: PMC3334321. doi: 10.1038/nprot.2012.016 PMID: 22383036

18. Cheng SX, Okuda M, Hall A, Geibel JP, Hebert SC. Expression of calcium-sensing receptor in rat colonic epithelium: evidence for modulation of fluid secretion. The American journal of physiology. 2002; 283:G240–50.

19. Gilda JE, Gomes AV. Stain-Free total protein staining is a superior loading control to beta-actin for Western blots. Analytical biochemistry. 2013; 440(2):186–8. PubMed Central PMCID: PMC3809032. doi: 10.1016/j.ab.2013.05.027 PMID: 23747530

20. Zhang ZR, Zeltwanger S, McCarty NA. Direct comparison of NPPB and DPC as probes of CFTR expressed in Xenopus oocytes. The Journal of membrane biology. 2000; 175(1):35–52. PMID: 10811966

21. Zhu JX, Zhang GH, Yang N, Rowlands DK, Wong HY, Tsang LL, et al. Activation of apical CFTR and basolateral Ca(2+)-activated K+ channels by tetramethylpyrazine in Caco-2 cell line. European journal of pharmacology. 2005; 510(3):187–95. doi: 10.1016/j.ejphar.2005.01.026 PMID: 15763242

22. Sheppard DN, Robinson KA. Mechanism of glibenclamide inhibition of cystic fibrosis transmembrane conductance regulator Cl- channels expressed in a murine cell line. The Journal of physiology. 1997; 503 (Pt 2):333–46. PubMed Central PMCID: PMC1159866.

23. Zhu JX, Xue H, Ji T, Xing Y. Cellular localization of NKCC2 and its possible role in the Cl- absorption in the rat and human distal colonic epithelia. Translational research: the journal of laboratory and clinical medicine. 2011; 158(3):146–54.

24. Gillen CM, Brill S, Payne JA, Forbush B 3rd. Molecular cloning and functional expression of the K-Cl cotransporter from rabbit, rat, and human. A new member of the cation-chloride cotransporter family. The Journal of biological chemistry. 1996; 271(27):16237–44. PMID: 8663127

25. Sangan P, Brill SR, Sangan S, Forbush B 3rd, Binder HJ. Basolateral K-Cl cotransporter regulates colonic potassium absorption in potassium depletion. The Journal of biological chemistry. 2000; 275 (40):30813–6. doi: 10.1074/jbc.M003931200 PMID: 10878016

26. Gamba G, Saltzberg SN, Lombardi M, Miyanoshita A, Lytton J, Hediger MA, et al. Primary structure and functional expression of a cDNA encoding the thiazide-sensitive, electroneutral sodium-chloride cotransporter. Proceedings of the National Academy of Sciences of the United States of America. 1993; 90(7):2749–53. PubMed Central PMCID: PMC46173. PMID: 8464884

27. Alrefai WA, Wen X, Jiang W, Katz JP, Steinbrecher KA, Cohen MB, et al. Molecular cloning and pro-moter analysis of downregulated in adenoma (DRA). American journal of physiology Gastrointestinal and liver physiology. 2007; 293(5):G923–34. doi: 10.1152/ajpgi.00029.2007 PMID: 17761837

28. Ohana E, Yang D, Shcheynikov N, Muallem S. Diverse transport modes by the solute carrier 26 family of anion transporters. The Journal of physiology. 2009;587(Pt 10):2179–85. PubMed Central PMCID: PMC2697291.

29. Reddy MM, Quinton PM. Intracellular Cl activity: evidence of dual mechanisms of cl absorption in sweat duct. The American journal of physiology. 1994; 267(4 Pt 1):C1136–44.

30. Larsen EH. Chloride transport by high-resistance heterocellular epithelia. Physiological reviews. 1991; 71(1):235–83. PMID: 1986389

31. Pech V, Kim YH, Weinstein AM, Everett LA, Pham TD, Wall SM. Angiotensin II increases chloride absorption in the cortical collecting duct in mice through a pendrin-dependent mechanism. American journal of physiology Renal physiology. 2007; 292(3):F914–20. doi: 10.1152/ajprenal.00361.2006 PMID: 17077386

32. Voute CL, Meier W. The mitochondria-rich cell of frog skin as hormone-sensitive "shunt-path". The Jour-nal of membrane biology. 1978; 40 Spec No:151–65. PMID: 215770

33. Rossier BC, Baker ME, Studer RA. Epithelial sodium transport and its control by aldosterone: the story of our internal environment revisited. Physiological reviews. 2015; 95(1):297–340. doi: 10.1152/physrev.00011.2014 PMID: 25540145

34. Cheng SX. Calcium-sensing receptor: A new target for therapy of diarrhea. World J Gastroenterol. 2016; 22(9):2711–24. PubMed Central PMCID: PMC4777994. doi: 10.3748/wjg.v22.i9.2711 PMID: 26973410

35. Hebert S, Cheng S, Geibel J. Functions and roles of the extracellular Ca2+sensing receptor in the gas-trointestinal tract. Cell calcium. 2004; 35(3):239–47. PMID: 15200147

36. Tang L, Cheng CY, Sun X, Pedicone AJ, Mohamadzadeh M, Cheng SX. The Extracellular Calcium-Sensing Receptor in the Intestine: Evidence for Regulation of Colonic Absorption, Secretion, Motility, and Immunity. Front Physiol. 2016; 7:245. doi: 10.3389/fphys.2016.00245 PMID: 27458380

37. Cheng SX, Geibel J, Hebert S. Extracellular polyamines regulate fluid secretion in rat colonic crypts via the extracellular calcium-sensing receptor. Gastroenterology. 2004; 126(1):148–58. PMID: 14699496

38. Geibel J, Sritharan K, Geibel R, Geibel P, Persing JS, Seeger A, et al. Calcium-sensing receptor abro-gates secretagogue-induced increases in intestinal net fluid secretion by enhancing cyclic nucleotide destruction. Proc Natl Acad Sci USA. 2006; 103(25):9390–7. doi: 10.1073/pnas.0602996103 PMID: 16760252

39. Joiner WJ, Basavappa S, Vidyasagar S, Nehrke K, Krishnan S, Binder HJ, et al. Active K+ secretion through multiple KCa-type channels and regulation by IKCa channels in rat proximal colon. American journal of physiology Gastrointestinal and liver physiology. 2003; 285(1):G185–96. doi: 10.1152/ajpgi.00337.2002 PMID: 12606302

40. Rajendran VM, Singh SK, Geibel J, Binder HJ. Differential localization of colonic H(+)-K(+)-ATPase iso-forms in surface and crypt cells. The American journal of physiology. 1998; 274(2 Pt 1):G424–9.

41.   Foster ES, Sandle GI, Hayslett JP, Binder HJ. Dietary potassium modulates active potassium absorp-
       tion and secretion in rat distal colon. The American journal of physiology. 1986; 251(5 Pt 1):G619–26.

42.   Rajendran VM, Binder HJ. Characterization of Na-H exchange in apical membrane vesicles of rat colon.
       The Journal of biological chemistry. 1990; 265(15):8408–14. PMID: 2160456

43.   Cho JH, Musch MW, Bookstein CM, McSwine RL, Rabenau K, Chang EB. Aldosterone stimulates intes-
       tinal Na+ absorption in rats by increasing NHE3 expression of the proximal colon. The American journal
       of physiology. 1998; 274(3 Pt 1):C586–94.

44.   Rajendran VM, Kashgarian M, Binder HJ. Aldosterone induction of electrogenic sodium transport in the
       apical membrane vesicles of rat distal colon. The Journal of biological chemistry. 1989; 264(31):18638–
       44. PMID: 2553716